

3D Relativistic Hartree-Bogoliubov model with a separable pairing interaction

T. Nikšić and D. Vretenar

*Physics Department, Faculty of Science,
University of Zagreb, 10000 Zagreb, Croatia*

Yuan Tian and Zhong-yu Ma

China Institute of Atomic Energy, Beijing 102413, People's Republic of China

P. Ring

Physik-Department der Technischen Universität München, D-85748 Garching, Germany

(Dated: October 30, 2018)

Abstract

A recently introduced separable pairing force for relativistic Hartree-Bogoliubov (RHB) calculations, adjusted in nuclear matter to the pairing gap of the Gogny force, is employed in the 3D RHB model for triaxial shapes. The pairing force is separable in momentum space but, when transformed to coordinate space in calculations of finite nuclei, it is no longer separable because of translational invariance. The corresponding pairing matrix elements are represented as a sum of a finite number of separable terms in the basis of a 3D harmonic oscillator. The 3D RHB model is applied to the calculation of binding energy surfaces and pairing energy maps for a sequence of even-A Sm isotopes.

PACS numbers: 21.60.Jz, 21.60.Ev, 21.10.Re, 21.10.Ky

I. INTRODUCTION

The structure of heavy complex nuclei with a large number of active valence nucleons is, at present, best described by the framework of nuclear energy density functionals (NEDF). A variety of structure phenomena, not only in stable nuclei, but also in regions of nuclei far from the valley of β -stability and close to the nucleon drip-lines, have been described with self-consistent mean-field models based on the Gogny interaction, the Skyrme energy functional, and the relativistic meson-exchange effective Lagrangians [1, 2].

Self-consistent relativistic mean-field (RMF) models have been employed in analyses of properties of ground and excited states in spherical and deformed nuclei. For a quantitative analysis of open-shell nuclei it is necessary to consider also pairing correlations. Pairing has often been taken into account in a very phenomenological way in the BCS model with the monopole pairing force, adjusted to the experimental odd-even mass differences. In many cases, however, this approach presents only a poor approximation. The physics of weakly-bound nuclei, in particular, necessitates a unified and self-consistent treatment of mean-field and pairing correlations. This has led to the formulation and development of the relativistic Hartree-Bogoliubov (RHB) model, which represents a relativistic extension of the conventional Hartree-Fock-Bogoliubov framework. In most applications of the RHB model [2] the pairing part of the Gogny force [3] has been employed in the particle-particle (pp) channel:

$$V^{pp}(1,2) = \sum_{i=1,2} e^{-((\mathbf{r}_1-\mathbf{r}_2)/\mu_i)^2} (W_i + B_i P^\sigma - H_i P^\tau - M_i P^\sigma P^\tau), \quad (1)$$

with the set D1S [4] for the parameters μ_i , W_i , B_i , H_i , and M_i ($i = 1, 2$). A basic advantage of the Gogny force is the finite range, which automatically guarantees a proper cut-off in momentum space. However, the resulting pairing field is non-local and the solution of the corresponding Dirac-Hartree-Bogoliubov integro-differential equations can be time-consuming, especially in the case of deformed nuclei. An alternative is the use of a zero-range, possibly density-dependent, δ -force in the pp -channel of the RHB model [5], but this approach introduces an additional cut-off parameter in energy. The effective range of the pairing interaction is determined by the energy cut-off, and the strength parameter must be chosen accordingly in order to reproduce empirical pairing gaps. In Ref. [6] we have implemented a renormalization scheme for the relativistic Hartree-Bogoliubov equations with

a zero-range pairing interaction. The procedure is equivalent to a simple energy cut-off with a position dependent coupling constant, and the resulting average pairing gaps and pairing energies do not depend on the cut-off energy. A density-dependent strength parameter of the zero-range pairing can be adjusted in such a way that the renormalization procedure reproduces in symmetric nuclear matter the pairing gap of the Gogny force Eq. (1).

In a series of recent articles [7, 8, 9] we have introduced a separable form of the pairing force for RHB calculations in spherical and axially deformed nuclei. The force is separable in momentum space, and is completely determined by two parameters that are adjusted to reproduce in symmetric nuclear matter the bell-shape curve of the pairing gap of the Gogny force. Technically this approach is similar to the derivation of non-empirical pairing functionals from low-momentum interactions [10, 11]. In applications to finite nuclei, when transformed from momentum to coordinate space, the pairing force is no longer separable because of translational invariance. It has been shown, however, that a method developed by Talmi and Moshinsky can be used to represent the corresponding pp matrix elements as a sum of a finite number of separable terms. When the nucleon wave functions are expanded in a harmonic oscillator basis, spherical or axially deformed, the sum converges relatively quickly, i.e. a reasonably small number of separable terms reproduces with high accuracy the results of calculations performed in a complete basis.

The simple separable force considered in Refs. [7, 8, 9] reproduces pairing properties of spherical and axially deformed nuclei calculated with the original Gogny force, but with the important advantage that the computational cost is greatly reduced. In the present work we extend this approach to triaxial nuclei, and introduce a 3D RHB model with the separable pairing interaction of Ref. [7] in the pp channel. This model will enable systematic calculations of RHB binding energy surfaces in the $\beta - \gamma$ plane, based on relativistic nuclear energy density functionals, that can be used as input for the generator coordinate method configuration mixing of angular-momentum projected triaxial wave functions, or to determine the parameters of a five-dimensional collective Hamiltonian for quadrupole vibrational and rotational degrees of freedom [12]. In Sec. II we introduce the 3D RHB model and derive the pp matrix element of the pairing force as a sum of a finite number of separable terms in the basis of a 3D harmonic oscillator. Illustrative calculations for even- A Sm isotopes are presented in In Sec. III. Section IV summarizes the results and ends with an outlook for future applications. Details on the expansion of single-nucleon spinors in the 3D harmonic

oscillator basis, and the transformation of the product of harmonic oscillator wave functions to the center-of-mass frame, are included in the two appendixes.

II. 3D RELATIVISTIC HARTREE-BOGOLIUBOV MODEL WITH A SEPARABLE PAIRING INTERACTION

The relativistic Hartree-Bogoliubov framework [2] provides a unified description of particle-hole (ph) and particle-particle (pp) correlations on a mean-field level by using two average potentials: the self-consistent mean field that encloses all the long range ph correlations, and a pairing field $\hat{\Delta}$ which sums up the pp -correlations. The ground state of a nucleus is described by a generalized Slater determinant $|\Phi\rangle$ that represents the vacuum with respect to independent quasiparticles. The quasiparticle operators are defined by the unitary Bogoliubov transformation of the single-nucleon creation and annihilation operators:

$$\alpha_k^+ = \sum_l U_{lk} c_l^+ + V_{lk} c_l, \quad (2)$$

where U and V are the Hartree-Bogoliubov wave functions determined by the solution of the RHB equation. In coordinate representation:

$$\begin{pmatrix} h_D - m - \lambda & \Delta \\ -\Delta^* & -h_D^* + m + \lambda \end{pmatrix} \begin{pmatrix} U_k(\mathbf{r}) \\ V_k(\mathbf{r}) \end{pmatrix} = E_k \begin{pmatrix} U_k(\mathbf{r}) \\ V_k(\mathbf{r}) \end{pmatrix}. \quad (3)$$

In the relativistic case the self-consistent mean-field corresponds to the single-nucleon Dirac Hamiltonian \hat{h}_D . In the usual σ , ω , and ρ meson-exchange representation, and for the stationary case with time-reversal symmetry, i.e. for the ground-state of an even-even nucleus:

$$\hat{h}_D = -i\boldsymbol{\alpha}\boldsymbol{\nabla} + \beta(m + g_\sigma\sigma(\mathbf{r})) + g_\omega\omega^0(\mathbf{r}) + g_\rho\tau_3\rho^0(\mathbf{r}) + e\frac{1-\tau_3}{2}A^0(\mathbf{r}). \quad (4)$$

The classical meson fields are solutions of the stationary Klein-Gordon equations:

$$[-\Delta + m_\sigma^2] \sigma(\mathbf{r}) = -g_\sigma(\rho)\rho_s(\mathbf{r}), \quad (5)$$

$$[-\Delta + m_\omega^2] \omega^0(\mathbf{r}) = g_\omega(\rho)\rho(\mathbf{r}), \quad (6)$$

$$[-\Delta + m_\rho^2] \rho^0(\mathbf{r}) = g_\rho(\rho)\rho_3^0(\mathbf{r}), \quad (7)$$

$$-\Delta A^0(\mathbf{r}) = \rho_p(\mathbf{r}), \quad (8)$$

for the σ meson, the time-like components of the ω meson and ρ meson, and the Poisson equation for the vector potential, respectively. In the general case when the meson-nucleon

couplings g_σ , g_ω , and g_ρ explicitly depend on the nucleon (vector) density ρ , there is an additional contribution to the nucleon self-energy - the rearrangement term [2], essential for the energy-momentum conservation and the thermodynamical consistency of the model.

In Eq. (3) m is the nucleon mass, and the chemical potential λ is determined by the particle number subsidiary condition in order that the expectation value of the particle number operator in the ground state equals the number of nucleons. The pairing field Δ reads

$$\Delta_{ab}(\mathbf{r}, \mathbf{r}') = \frac{1}{2} \sum_{c,d} V_{abcd}(\mathbf{r}, \mathbf{r}') \kappa_{cd}(\mathbf{r}, \mathbf{r}'). \quad (9)$$

where $V_{abcd}(\mathbf{r}, \mathbf{r}')$ are the matrix elements of the two-body pairing interaction, and the indices a , b , c and d denote the quantum numbers that specify the Dirac indices of the spinor. The column vectors denote the quasiparticle wave functions, and E_k are the quasiparticle energies. The dimension of the RHB matrix equation is two times the dimension of the corresponding Dirac equation. For each eigenvector (U_k, V_k) with positive quasiparticle energy $E_k > 0$, there exists an eigenvector (V_k^*, U_k^*) with quasiparticle energy $-E_k$. Since the baryon quasiparticle operators satisfy fermion commutation relations, the levels E_k and $-E_k$ cannot be occupied simultaneously. For the solution that corresponds to a ground state of a nucleus with even particle number, one usually chooses the eigenvectors with positive eigenvalues E_k .

The single-particle density and the pairing tensor, constructed from the quasi-particle wave functions

$$\rho_{cd}(\mathbf{r}, \mathbf{r}') = \sum_{k>0} V_{ck}^*(\mathbf{r}) V_{dk}(\mathbf{r}'), \quad (10)$$

$$\kappa_{cd}(\mathbf{r}, \mathbf{r}') = \sum_{k>0} U_{ck}^*(\mathbf{r}) V_{dk}(\mathbf{r}'), \quad (11)$$

are calculated in the *no-sea* approximation (denoted by $k > 0$): the summation runs over all quasiparticle states k with positive quasiparticle energies $E_k > 0$, but omits states that originate from the Dirac sea. The latter are characterized by a quasiparticle energy larger than the Dirac gap (≈ 1200 MeV).

Pairing correlations in nuclei are restricted to an energy window of a few MeV around the Fermi level, and their scale is well separated from the scale of binding energies, which are in the range of several hundred to thousand MeV. There is no empirical evidence for any relativistic effect in the nuclear pairing field $\hat{\Delta}$ and, therefore, a hybrid RHB model with a

non-relativistic pairing interaction can be formulated. For a general two-body interaction, the matrix elements of the relativistic pairing field read

$$\hat{\Delta}_{a_1 p_1, a_2 p_2} = \frac{1}{2} \sum_{a_3 p_3, a_4 p_4} \langle a_1 p_1, a_2 p_2 | V^{pp} | a_3 p_3, a_4 p_4 \rangle_a \kappa_{a_3 p_3, a_4 p_4}, \quad (12)$$

where the indices ($p_1, p_2, p_3, p_4 \equiv f, g$) refer to the large and small components of the quasi-particle Dirac spinors:

$$U(\mathbf{r}, s, t) = \begin{pmatrix} f_U(\mathbf{r}, s, t) \\ ig_U(\mathbf{r}, s, t) \end{pmatrix} \quad V(\mathbf{r}, s, t) = \begin{pmatrix} f_V(\mathbf{r}, s, t) \\ ig_V(\mathbf{r}, s, t) \end{pmatrix}. \quad (13)$$

In practical applications of the RHB model to finite open-shell nuclei, only the large components of the spinors $U_k(\mathbf{r})$ and $V_k(\mathbf{r})$ are used to build the non-relativistic pairing tensor $\hat{\kappa}$ in Eq. (11). The resulting pairing field reads

$$\hat{\Delta}_{a_1 f, a_2 f} = \frac{1}{2} \sum_{a_3 f, a_4 f} \langle a_1 f, a_2 f | V^{pp} | a_3 f, a_4 f \rangle_a \kappa_{a_3 f, a_4 f}. \quad (14)$$

The other components: $\hat{\Delta}_{fg}$, $\hat{\Delta}_{gf}$, and $\hat{\Delta}_{gg}$ can be safely omitted [13].

The Dirac-Hartree-Bogoliubov equations and the equations for the meson fields are solved by expanding the nucleon spinors $U(\mathbf{r}, s, t)$ and $V(\mathbf{r}, s, t)$, and the meson fields, in the basis of a three-dimensional harmonic oscillator (HO) in Cartesian coordinates. In this way both axial and triaxial nuclear shapes can be described. In addition, to reduce the computational task, it is assumed that the total densities are symmetric under reflections with respect to all three planes xy , xz and yz . When combined with time-reversal invariance, this also implies that parity is conserved. The single-nucleon basis is defined in Appendix A.

In Ref. [7] a new separable form of the pairing interaction has been introduced, with parameters adjusted to reproduce the pairing properties of the Gogny force in nuclear matter. The gap equation in the 1S_0 channel reads

$$\Delta(k) = - \int_0^\infty \frac{k'^2 dk'}{2\pi^2} \langle k | V^{1S_0} | k' \rangle \frac{\Delta(k')}{2E(k')}, \quad (15)$$

and the pairing force is separable in momentum space:

$$\langle k | V^{1S_0} | k' \rangle = -Gp(k)p(k'). \quad (16)$$

By assuming a simple Gaussian ansatz $p(k) = e^{-a^2 k^2}$, the two parameters G and a have been adjusted to reproduce the density dependence of the gap at the Fermi surface, calculated with

a Gogny force. For the D1S parameterization [4] of the Gogny force: $G = -728 \text{ MeVfm}^3$ and $a = 0.644 \text{ fm}$. When the pairing force Eq. (16) is transformed from momentum to coordinate space, it takes the form:

$$V(\mathbf{r}_1, \mathbf{r}_2, \mathbf{r}'_1, \mathbf{r}'_2) = G \delta(\mathbf{R} - \mathbf{R}') P(\mathbf{r}) P(\mathbf{r}') \frac{1}{2} (1 - P^\sigma), \quad (17)$$

where $\mathbf{R} = \frac{1}{2}(\mathbf{r}_1 + \mathbf{r}_2)$ and $\mathbf{r} = \mathbf{r}_1 - \mathbf{r}_2$ denote the center-of-mass and the relative coordinates, and $P(\mathbf{r})$ is the Fourier transform of $p(k)$:

$$P(\mathbf{r}) = \frac{1}{(4\pi a^2)^{3/2}} e^{-\mathbf{r}^2/4a^2}. \quad (18)$$

The pairing force has finite range and, because of the presence of the factor $\delta(\mathbf{R} - \mathbf{R}')$, it preserves translational invariance. Even though $\delta(\mathbf{R} - \mathbf{R}')$ implies that this force is not completely separable in coordinate space, the corresponding pp matrix elements can be represented as a sum of a finite number of separable terms in the basis of a 3D harmonic oscillator:

$$V_{\alpha\beta\gamma\delta}^{pp} = \sum_{N_x=0}^{N_x^0} \sum_{N_y=0}^{N_y^0} \sum_{N_z=0}^{N_z^0} V_{\alpha\beta}^{N_x N_y N_z} V_{\gamma\delta}^{N_x N_y N_z}, \quad (19)$$

where N_x , N_y , and N_z are the quantum numbers of the corresponding 1D HOs in the center-of-mass frame (cf. Appendix B). This means that the pairing field can also be written as a sum of a finite number of separable terms:

$$\Delta_{\alpha\beta} = \frac{1}{2} \sum_{N_x=0}^{N_x^0} \sum_{N_y=0}^{N_y^0} \sum_{N_z=0}^{N_z^0} P_{N_x N_y N_z} V_{\alpha\beta}^{N_x N_y N_z}, \quad (20)$$

with the coefficients

$$P_{N_x N_y N_z} = \sum_{\gamma\delta} V_{\gamma\delta}^{N_x N_y N_z} \kappa_{\gamma\delta}. \quad (21)$$

The advantage of using the separable pairing interaction Eq. (17) is that the matrices $V_{\alpha\beta}^{N_x N_y N_z}$ are calculated only once at the beginning of a self-consistent calculation. The coefficients $P_{N_x N_y N_z}$ are re-calculated at each iteration step, using the corresponding updated pairing tensor κ .

In the following we calculate the antisymmetric matrix element of the pairing interaction Eq. (17)

$$\langle \alpha\bar{\gamma} | V | \beta\bar{\delta} \rangle_a = \langle \alpha\bar{\gamma} | V | \beta\bar{\delta} \rangle - \langle \alpha\bar{\gamma} | V | \bar{\delta}\beta \rangle, \quad (22)$$

in the basis of a 3D harmonic oscillator, where $|\alpha\rangle$ and $|\bar{\alpha}\rangle$ denote the positive and negative x-simplex operator eigenstates (cf. Appendix A)

$$|\alpha\rangle \equiv |n_x^\alpha n_y^\alpha n_z^\alpha; i = +\rangle = |n^\alpha\rangle \frac{i^{n_y^\alpha}}{\sqrt{2}} [|\uparrow\rangle - (-1)^{n_x^\alpha} |\downarrow\rangle], \quad (23)$$

$$|\bar{\alpha}\rangle \equiv |n_x^\alpha n_y^\alpha n_z^\alpha; i = -\rangle = |n^\alpha\rangle \frac{i^{n_y^\alpha}}{\sqrt{2}} (-1)^{n_x^\alpha + n_y^\alpha + 1} [|\uparrow\rangle + (-1)^{n_x^\alpha} |\downarrow\rangle]. \quad (24)$$

The matrix element can be separated into a product of spin and coordinate space factors

$$\langle \alpha \bar{\gamma} | V | \beta \bar{\delta} \rangle_a = \langle \alpha \bar{\gamma} | W \frac{1}{2} (1 - P^\sigma) | \beta \bar{\delta} \rangle_a. \quad (25)$$

The operator $\frac{1}{2}(1 - P^\sigma)$ projects onto the $S = 0$ spin-singlet product state

$$|\beta \bar{\delta}\rangle_{S=0} = -|\bar{\delta}\beta\rangle_{S=0} = \frac{1}{4} i^{n_y^\delta + n_y^\beta} (-1)^{n_y^\delta + 1} \left[1 + (-1)^{n_x^\beta + n_x^\delta} \right] [|\uparrow\downarrow\rangle - |\downarrow\uparrow\rangle] |n^\beta n^\delta\rangle, \quad (26)$$

and the problem is reduced to the calculation of the spatial part of the matrix element

$$\langle \alpha \bar{\gamma} | V | \beta \bar{\delta} \rangle_a = \frac{1}{8} i^{n_y^\alpha + n_y^\beta + n_y^\gamma + n_y^\delta} (-1)^{n_y^\alpha + n_y^\delta} \left[1 + (-1)^{n_x^\beta + n_x^\delta} \right] \left[1 + (-1)^{n_x^\alpha + n_x^\gamma} \right] \times \quad (27)$$

$$\times \left[\langle n^\alpha n^\gamma | W | n^\beta n^\delta \rangle + \langle n^\alpha n^\gamma | W | n^\delta n^\beta \rangle \right]. \quad (28)$$

For $W(\mathbf{r}_1, \mathbf{r}_2, \mathbf{r}'_1, \mathbf{r}'_2) = G\delta(\mathbf{R} - \mathbf{R}')P(\mathbf{r})P(\mathbf{r}')$ (cf. Eq. (17)), the spatial part of the matrix element

$$I \equiv \int \phi_{n_x^\alpha}(\mathbf{r}_1) \phi_{n_x^\gamma}(\mathbf{r}_2) W(\mathbf{r}_1, \mathbf{r}_2, \mathbf{r}'_1, \mathbf{r}'_2) \phi_{n_x^\beta}(\mathbf{r}'_1) \phi_{n_x^\delta}(\mathbf{r}'_2) d\mathbf{r}_1 d\mathbf{r}_2 d\mathbf{r}'_1 d\mathbf{r}'_2, \quad (29)$$

can be decomposed into three Cartesian components

$$I = GI_x I_y I_z. \quad (30)$$

Here we only derive a detailed expression for the x -component

$$I_x = \int \phi_{n_x^\alpha}(x_1, b_x) \phi_{n_x^\gamma}(x_2, b_x) P(x) \delta(X - X') P(x') \phi_{n_x^\beta}(x'_1, b_x) \phi_{n_x^\delta}(x'_2, b_x) dx_1 dx_2 dx'_1 dx'_2. \quad (31)$$

We will use the transformation of a product of 1D HO wave functions to the center-of-mass and relative coordinates, derived in Eq. (B20)

$$\phi_{n_x^\alpha}(x_1, b_x) \phi_{n_x^\gamma}(x_2, b_x) = \sum_{N_x, n_x} M_{n_x^\alpha n_x^\gamma}^{n_x N_x} \phi_{N_x}(X, B) \phi_{n_x}(x, b_{x,r}), \quad (32)$$

$$\phi_{n_x^\beta}(x'_1, b_x) \phi_{n_x^\delta}(x'_2, b_x) = \sum_{N'_x, n'_x} M_{n_x^\beta n_x^\delta}^{n'_x N'_x} \phi_{N'_x}(X', B) \phi_{n'_x}(x', b_{x,r}). \quad (33)$$

The volume element in Eq. (31) is transformed:

$$dx_1 dx_2 dx'_1 dx'_2 = -dX dX' dx dx'. \quad (34)$$

The integral Eq. (31) now reads

$$\begin{aligned} I_x = & - \sum_{N_x, n_x} M_{n_\alpha^x n_\gamma^x}^{n_x N_x} \sum_{N'_x, n'_x} M_{n_\beta^x n_\delta^x}^{n'_x N'_x} \int P(x) \phi_{n_x}(x, b_{x,r}) dx \int P(x') \phi_{n'_x}(x', b_{x,r}) dx' \times \\ & \times \iint \delta(X - X') \phi_{N_x}(X, B) \phi_{N'_x}(X', B) dX dX'. \end{aligned} \quad (35)$$

By making use of:

$$\iint \delta(X - X') \phi_{N_x}(X, B) \phi_{N'_x}(X', B) dX dX' = \int \phi_{N_x}(X, B) \phi_{N'_x}(X, B) dX = \delta_{N_x, N'_x}, \quad (36)$$

the integral can be written in the form

$$I_x = - \sum_{N_x} M_{n_\alpha^x n_\gamma^x}^{n_x N_x} M_{n_\beta^x n_\delta^x}^{n'_x N'_x} I_{n_x}(b_{x,r}) I_{n'_x}(b_{x,r}), \quad (37)$$

where I_{n_x} denotes

$$I_{n_x}(b_{x,r}) = \int P(x) \phi_{n_x}(x, b_{x,r}) dx. \quad (38)$$

Note that the conditions

$$n_\alpha^x + n_\gamma^x = n_x + N_x \quad \text{and} \quad n_\beta^x + n_\delta^x = n'_x + N'_x, \quad (39)$$

have been used to eliminate the sums over n_x and n'_x . To evaluate the integral $I_{n_x}(b_{x,r})$, we make use of the generating function for the HO wave functions Eq. (B2), and calculate the following integral:

$$J(p, b) = \int_{-\infty}^{\infty} g(x, p, b) P(x) dx = \pi^{-1/4} \sqrt{\frac{b}{b^2 + 2a^2}} \sum_{n=0}^{\infty} (-1)^n \left(\frac{b^2 - 2a^2}{b^2 + 2a^2} \right)^n p^{2n}. \quad (40)$$

Using the definition of the generating function Eq. (B2), this expression can also be written as follows

$$J(p, b) = \sum_{n=0}^{\infty} p^{2n} \sqrt{\frac{2^{2n}}{(2n)!}} \int_{-\infty}^{\infty} P(x) \phi_{2n}(x, b) dx. \quad (41)$$

The series contains only even powers because $P(x)$ is a symmetric function. By comparing Eqs. (40) and (41), we obtain

$$\int_{-\infty}^{\infty} P(x) \phi_n(x, b) dx = \pi^{-1/4} \sqrt{\frac{b}{b^2 + 2a^2}} (-1)^{n/2} \left(\frac{b^2 - 2a^2}{b^2 + 2a^2} \right)^{n/2} \delta_{n, \text{even}}, \quad (42)$$

and finally, inserting the relative oscillator length $b_r = \sqrt{2}b$ (cf. Appendix B) ,

$$I_{n_x}(b_{x,r}) = \frac{1}{(2\pi)^{1/4}} \sqrt{\frac{b}{b^2 + a^2}} (-1)^{n/2} \left(\frac{b^2 - a^2}{b^2 + a^2} \right)^{n/2} \delta_{n,even} . \quad (43)$$

The number of terms in Eq. (37) and then, of course, in Eqs. (19) and (20) is in principle limited by the dimension of the oscillator basis. If single-particle oscillator states $|n_x n_y n_z\rangle$ with $n_x + n_y + n_z \leq N_f^{max}$ form the basis, the summation over the quantum number of the 1D HO in the center-of-mass frame in Eq. (37) runs over $N_x = 0, \dots, 2N_f^{max}$. This means that the maximal total number of terms in Eqs. (19) and (20) equals $N_{tot}^{max} = (2N_f^{max} + 1)^3$. However, results of calculations performed in Refs. [7, 9] suggest that the actual number of terms that give significant contributions to the pairing field is much smaller. If a cut-off condition is imposed

$$N_x \leq N_x^c, \quad N_y \leq N_y^c, \quad N_z \leq N_z^c, \quad (44)$$

the total number of separable terms becomes:

$$N_{sep} = \frac{1}{8} (N_x^c + 2) (N_y^c + 2) (N_z^c + 2) . \quad (45)$$

In the next section we will compare some results of illustrative 3D RHB calculations with those obtained assuming axial symmetry [9]. For a meaningful comparison with results calculated using the axial RHBZ code [9], we will make the following choice: $N_x + N_y \leq N_\perp^c$ and $N_z \leq N_z^c$. In this case the total number of separable terms equals

$$N_{sep}^{axial} = \frac{1}{8} (N_\perp^c + 1)^2 (N_z^c + 2) . \quad (46)$$

III. ILLUSTRATIVE CALCULATIONS

In this section we present the results of illustrative 3D RHB calculations for a sequence of Sm isotopes. The separable pairing force Eq. (17) is used in the pp channel, and the mean field is determined by the density-dependent meson-exchange effective interaction DD-ME2 [14] in the ph channel. DD-ME2 has been adjusted to empirical properties of symmetric and asymmetric nuclear matter, binding energies, charge radii, and neutron radii of spherical nuclei. The interaction has been tested in calculations of ground state properties of large set of spherical and deformed nuclei. An excellent agreement with data has been obtained for binding energies, charge isotope shifts, and quadrupole deformations. When

used in the relativistic RPA, DD-ME2 reproduces with high accuracy data on isoscalar and isovector collective excitations [14, 15].

In Figs. 1 and 2 we display the self-consistent RHB triaxial quadrupole binding energy maps of the $^{134-156}\text{Sm}$ isotopes in the $\beta - \gamma$ plane ($0^0 \leq \gamma \leq 60^0$). The map of the energy surface as a function of the quadrupole deformation is obtained by imposing constraints on the axial and triaxial quadrupole moments. The method of quadratic constraint uses an unrestricted variation of the function

$$\langle \hat{H} \rangle + \sum_{\mu=0,2} C_{2\mu} \left(\langle \hat{Q}_{2\mu} \rangle - q_{2\mu} \right)^2, \quad (47)$$

where $\langle \hat{H} \rangle$ is the total energy, and $\langle \hat{Q}_{2\mu} \rangle$ denotes the expectation value of the mass quadrupole operators:

$$\hat{Q}_{20} = 2z^2 - x^2 - y^2 \quad \text{and} \quad \hat{Q}_{22} = x^2 - y^2. \quad (48)$$

$q_{2\mu}$ is the constrained value of the multipole moment, and $C_{2\mu}$ the corresponding stiffness constant [16].

The energy maps shown in Figs. 1 and 2 nicely illustrate the gradual transition from the prolate and γ -soft deformed light isotopes $^{134,136}\text{Sm}$, through the spherical $N = 82$ neutron closed-shell nucleus ^{144}Sm , to the strongly prolate deformed, axial nuclei $^{154,156}\text{Sm}$. The isotopes below the $N = 82$ closed shell are all γ -soft and, just before the shell closure, one finds a slightly oblate minimum in ^{140}Sm . Sm nuclei with $N > 82$ quickly develop a pronounced prolate deformation, much stiffer with respect to the γ degree of freedom than isotopes below $N = 82$. Heavy Sm isotopes are characterized by axially symmetric shapes with pronounced prolate minima at $\beta > 0.3$.

The binding energy maps correspond to self-consistent solutions of the RHB equations, obtained by expanding the nucleon spinors and the meson fields in the basis of a three-dimensional harmonic oscillator (HO) in Cartesian coordinates. In the present calculation the basis includes $N_f^{max} = 14$ major oscillator shells. In Figs. 3 and 4 we plot the corresponding contour maps of the proton and neutron pairing energies in the $\beta - \gamma$ plane for the three lighter isotopes $^{134,136,138}\text{Sm}$, and for the three heavier nuclei $^{152,154,156}\text{Sm}$, respectively. Using the separable pairing force Eq. (17), the pairing field Eq. (20) is calculated as a sum of a finite number of separable terms. 3D calculations in the pp channel have been checked by comparing the results for the ground state properties of $^{134-154}\text{Sm}$, with those obtained

using the axial RHBZ code with the same separable pairing force [9], and with the pairing part of the original Gogny force [4, 17]. In the case when axial symmetry is assumed, the expansion for the pairing field runs over the quantum numbers N_z and N_p of the HO in the center-of-mass frame, corresponding to the z and ρ coordinates of the cylindrical coordinate system:

$$\Delta_{12} = -G \sum_{N_z}^{N_z^0} \sum_{N_p}^{N_p^0} W_{12}^{N_z N_p} P_{N_z} P_{N_p}. \quad (49)$$

The maximal values for the quantum numbers in the expansion of Dirac spinors are $n_z^0 = N_f^{max}$ and $n_p^0 = N_f^{max}/2$, i.e. the maximal values for the coefficients in expansion (49) are $N_z^0 = 2n_z^0 = 2N_f^{max}$ and $N_p^0 = 2n_p^0 = N_f^{max}$. In Ref. [9] it has been shown that, for axial calculations of prolate deformed nuclei, sufficient accuracy is achieved if the expansion of pairing matrix elements is limited to: $N_p \leq N_p^0 = 5$, and $N_z \leq N_z^0 = 14$. For this choice of the cut-off in the expansion of the pairing matrix elements in the basis of the HO in the center-of-mass frame, the resulting pairing energies reproduce to a very good approximation results obtained with the calculation in the full basis, and also those obtained with the Gogny force D1S in the pairing channel. In the present 3D calculation we have, therefore, imposed the following cut-off condition for the expansion in Eqs. (19), (20) and (21):

$$N_z = 0, 2, \dots, N_z^0 = 14 \quad \text{and} \quad N_x + N_y = 0, 2, \dots, 2N_p^0 = 5. \quad (50)$$

In Fig. 5 we display the 3D RHB ground-state binding energies for the Sm isotopes ($72 \leq N \leq 92$), in comparison with data from the compilation of Audi and Wapstra [18]. Calculations have also been performed with the axial RHBZ code [9], and the inset we plot the relative differences (in percent): $(E^{RHBZ} - E^{3DRHB})/E^{3DRHB}$, between the corresponding ground-state binding energies. As a further test, Fig. 6 compares the 3D RHB and axial (RHBZ) results for the self-consistent ground-state quadrupole deformations, neutron and proton pairing energies of even- A Sm isotopes. In calculations with axial symmetry (RHBZ) both the separable force and the Gogny D1S force [4] are used in the pairing channel. The excellent agreement between the three sets of results demonstrate not only the numerical accuracy of the new 3D computer code, but also show that using the separable pairing force in deformed nuclei, virtually identical pairing energies are calculated as with the original Gogny force.

IV. SUMMARY AND OUTLOOK

Realistic self-consistent mean-field calculations based on finite-range interactions, including exchange terms and/or pairing correlations, still present a considerable computational challenge [19, 20, 21, 22], particularly if one considers complex triaxial shapes or extensions beyond the simplest mean-field approximation. A great advantage of mean-field models based on Skyrme-like zero-range interactions is that they provide a simple and elegant treatment of Fock exchange and pairing terms [23, 24]. The disadvantage of such forces, i.e. the fact that they are constant in momentum space and can induce scattering of nucleons very high up into the continuum, does not appear at the Hartree or Hartree-Fock level, at which one considers only momenta up to the Fermi surface. In the pairing channel, however, because of the specific form of the BCS or Bogoliubov ansatz that takes into account pairing correlations on the mean-field level, ultraviolet divergencies occur for zero-range forces. One possible solution present the various cutoff procedures that have been used in the literature (cf. Ref. [25] and references therein). These approximations all include additional non-physical cut-off parameters. This does not cause any problem in investigations along the valley of beta-stability, where gap parameters can be deduced from experimental masses. However, the use of cut-off parameters limits the predictive power of such models in unknown regions of the nuclear chart, such as for superheavy elements or very neutron rich isotopes.

A completely different approach to the treatment of pairing correlations is the use of separable forces. A separable form of the pairing force for RHB calculations in finite nuclei has recently been introduced [7]. The force is separable in momentum space, and is completely determined by two parameters that are adjusted to reproduce in symmetric nuclear matter the bell-shape curve of the pairing gap of the Gogny force. Because of translational invariance, the pairing force is no longer exactly separable in coordinate space, but Talmi-Moshinsky techniques allow a simple transformation into a quickly converging series of separable terms in a harmonic oscillator basis. Although different from the Gogny force, the corresponding effective pairing interaction has been shown to reproduce with high accuracy pairing gaps and energies calculated with the original Gogny force, both in spherical and axially deformed nuclei. In particular, this approach retains the basic advantage of the finite-range Gogny force, i.e. the natural cut-off in momentum space.

Applications have so far been restricted to the description of spherical [7] and axially deformed nuclei [9]. In this work we have extended the model to describe triaxially deformed nuclei. The numerical accuracy of the new model has been analyzed by comparing results with those obtained in axially-symmetric calculations, using both the separable force as well as the original Gogny D1S force in the pairing channel.

To illustrate the applicability of this force in the description of realistic triaxial systems, we have explored the chain of Sm isotopes with $Z = 62$ protons, ranging from ^{134}Sm to ^{156}Sm . For the magic neutron number $N = 82$, i.e. for the ^{144}Sm isotope, a stable spherical minimum is found in the $\beta - \gamma$ plane. The two neighboring nuclei ^{142}Sm and ^{146}Sm are still spherical, but with much softer energy surfaces. In heavier isotopes we find a rather rapid transition to prolate shapes with a well pronounced minima, and increasing β -deformation up to $\beta \approx 0.3$. In these heavier nuclei we also find a soft saddle point on the oblate side, that eventually becomes a shallow second minimum in the isotope ^{156}Sm . Decreasing the neutron number below the closed shell at $N = 82$, a γ -soft valley develops with increasing β -deformation. For ^{140}Sm isotope we find a shallow oblate minimum, whereas for the lighter isotopes the minima are located on the prolate side, but the calculation predicts large fluctuations in the γ -direction.

One can envisage many possible applications of the separable pairing force. The force is simple enough to be applied in otherwise time consuming calculations, e.g. description of triaxial effects, rotating nuclei, fission process, spherical and deformed QRPA. It can also be used in various beyond mean-field extensions, such as restoration of broken symmetries, fluctuations of quadrupole moment and particle-vibration coupling. In the current version of the model, the pairing force has been adjusted to the pairing gap of the phenomenological Gogny D1S force. In the next step one could adjust the effective force to a pairing gap in nuclear matter calculated in a fully microscopic approach starting from inter-nucleon interactions [26, 27, 28].

ACKNOWLEDGMENTS

This work was supported in part by MZOS - project 1191005-1010, and by the DFG cluster of excellence ‘‘Origin and Structure of the Universe’’ (www.universe-cluster.de). T. N. acknowledges support from the Croatian National Foundation for Science. Y.T. and Z.Y.M. acknowledge support from the National Natural Science Foundation of China under Grants

10875150, 10775183, and 10535010, and the Major State Basis Research Development of China under Contract 2007CB815000.

APPENDIX A: THE SINGLE-NUCLEON BASIS

The Dirac single-nucleon spinors are expanded in the basis of eigenfunctions of a three-dimensional harmonic oscillator (HO) in Cartesian coordinates. In one dimension:

$$\phi_{n_\mu}(x_\mu) = b_\mu^{-1/2} \mathcal{N}_{n_\mu} H_{n_\mu}(\xi_\mu) e^{-\xi_\mu^2/2}, \quad (\mu \equiv x, y, z) \quad (\text{A1})$$

$\xi_\mu \equiv x_\mu/b_\mu$, and the oscillator length is defined as

$$b_\mu = \sqrt{\frac{\hbar}{m\omega_\mu}}. \quad (\text{A2})$$

The normalization factor reads

$$\mathcal{N}_n = \pi^{-1/4} (2^n n!)^{-1/2}, \quad (\text{A3})$$

and $H_n(\xi)$ denotes the Hermite polynomials [29]

$$\int_{-\infty}^{\infty} H_n(\xi) H_{n'}(\xi) e^{-\xi^2} d\xi = \delta_{nn'}. \quad (\text{A4})$$

The basis state can be defined as the product of three HO wave functions (one for each dimension) and the spin factor:

$$\phi_\alpha(\mathbf{r}; m_s) = \phi_{n_x}(\xi_x) \phi_{n_y}(\xi_y) \phi_{n_z}(\xi_z) \chi_{m_s}, \quad (\text{A5})$$

where the notation is: $\alpha \equiv \{n_x, n_y, n_z\}$. For each combination of quantum numbers $\{n_x, n_y, n_z\}$, the spin part is chosen in such a way that the basis state is an eigenfunction of the x-simplex operator $\hat{S}_x = \hat{P} e^{-i\pi \hat{J}_x}$, where \hat{P} denotes the parity operator. The positive and negative x-simplex operator eigenstates:

$$|n_x n_y n_z; i = +\rangle = |n_x n_y n_z\rangle \frac{i^{n_y}}{\sqrt{2}} [|\uparrow\rangle - (-1)^{n_x} |\downarrow\rangle], \quad (\text{A6})$$

$$|n_x n_y n_z; i = -\rangle = |n_x n_y n_z\rangle (-1)^{n_x + n_y + 1} \frac{i^{n_y}}{\sqrt{2}} [|\uparrow\rangle + (-1)^{n_x} |\downarrow\rangle], \quad (\text{A7})$$

are related by the time-reversal operator ($\hat{T} = i\sigma_y \hat{K}_0$)

$$|n_x n_y n_z; i = -\rangle = \hat{T} |n_x n_y n_z; i = +\rangle. \quad (\text{A8})$$

For the Dirac spinor with positive simplex eigenvalue, the large component corresponds to positive, and the small component to negative eigenvalues

$$\psi_i(\mathbf{r}, +) = \begin{pmatrix} f_i(\mathbf{r}, +) \\ ig_i(\mathbf{r}, -) \end{pmatrix}. \quad (\text{A9})$$

The large and small component are expanded in terms of the basis states Eqs. (A6) and (A7):

$$f_i(\mathbf{r}; +) = \sum_{\alpha}^{\alpha_{max}} f_i^{\alpha} \phi_{\alpha}(\mathbf{r}; +) \quad \text{and} \quad g_i(\mathbf{r}; -) = \sum_{\bar{\alpha}}^{\bar{\alpha}_{max}} g_i^{\bar{\alpha}} \phi_{\bar{\alpha}}(\mathbf{r}; -). \quad (\text{A10})$$

Positive simplex eigenstates are denoted by $|\alpha\rangle$, and negative simplex eigenstates by $|\bar{\alpha}\rangle$. If the basis states are arranged as: $\{\alpha_1, \dots, \alpha_M, \bar{\alpha}_1, \dots, \bar{\alpha}_M\}$, the x-simplex operator has a simple block-diagonal form, whereas the time-reversal operator is skew diagonal:

$$\hat{S}_x = i \begin{pmatrix} \mathbb{1} & 0 \\ 0 & -\mathbb{1} \end{pmatrix} \quad \text{and} \quad \hat{T} = \begin{pmatrix} 0 & \mathbb{1} \\ -\mathbb{1} & 0 \end{pmatrix}. \quad (\text{A11})$$

If the dimension of each simplex block ($i = \pm$) is M , the dimension of the entire configuration space equals $2M$. In the present implementation of the model parity is also conserved, and this allows a further reduction of the basis to four simplex-parity blocks. For a given maximal number of oscillator shells N_{max} , the dimension of the HO basis can be determined as follows. The states $|n_x n_y n_z\rangle$ within a major oscillator shell N are arranged as

n_x	n_y	n_z
0	0	N
0	1	$N - 1$
\vdots	\vdots	\vdots
0	N	0
1	0	$N - 1$
\vdots	\vdots	\vdots
1	$N - 1$	0
N	0	0

and the number of 3D HO basis states in the shell N then reads

$$n_{\text{states}}(N) = (N + 1) + N + (N - 1) + \dots + 1 = \frac{1}{2}(N + 1)(N + 2). \quad (\text{A12})$$

Because parity is conserved, the basis can be separated into positive and negative parity blocks. The dimension of the each block is determined by summing up the number of states in even/odd- N shells:

$$n_{\text{pos.}} = \frac{1}{2} \sum_{k=0}^{k_{\text{max}}^+} (2k+1)(2k+2) = \frac{1}{6} (k_{\text{max}}^+ + 1) (k_{\text{max}}^+ + 2) (4k_{\text{max}}^+ + 3), \quad (\text{A13})$$

$$n_{\text{neg.}} = \frac{1}{2} \sum_{k=0}^{k_{\text{max}}^-} (2k+2)(2k+3) = \frac{1}{6} (k_{\text{max}}^- + 1) (k_{\text{max}}^- + 2) (4k_{\text{max}}^- + 9), \quad (\text{A14})$$

where $k_{\text{max}}^+ = \lfloor N_{\text{max}}/2 \rfloor$ and $k_{\text{max}}^- = \lfloor (N_{\text{max}} - 1)/2 \rfloor$, and the square brackets denote integer division.

APPENDIX B: TRANSFORMATION OF THE PRODUCT OF 1D HO WAVE FUNCTIONS TO THE CENTER-OF-MASS FRAME

By multiplying the generating function for the Hermite polynomials

$$g(x, p, b) = e^{2xp/b-p^2} = \sum_{n=0}^{\infty} \frac{1}{n!} p^n H_n(x/b), \quad (\text{B1})$$

with the factor $\frac{1}{\sqrt{b}} \pi^{-1/4} e^{-x^2/2b^2}$, we obtain the generating function for the HO wave functions:

$$\frac{1}{\sqrt{b}} \pi^{-1/4} e^{-x^2/2b^2 + 2xp/b - p^2} = \sum_{n=0}^{\infty} \eta_n(p) \phi_n(x, b), \quad (\text{B2})$$

where $\eta_n(p)$ denotes

$$\eta_n(p) = p^n \sqrt{\frac{2^n}{n!}}. \quad (\text{B3})$$

For the product of two generating functions

$$g(x_1, p_1, b)g(x_2, p_2, b) = \frac{1}{b} \pi^{-1/2} e^{-\frac{1}{2b^2}(x_1^2 + x_2^2) + \frac{2}{b}(x_1 p_1 + x_2 p_2) - (p_1^2 + p_2^2)}, \quad (\text{B4})$$

a new set of coordinates is introduced:

$$\left. \begin{aligned} \tilde{x} &= \frac{1}{\sqrt{2}} (x_1 - x_2) \\ \tilde{X} &= \frac{1}{\sqrt{2}} (x_1 + x_2) \end{aligned} \right\} \iff \left\{ \begin{aligned} x_1 &= \frac{1}{\sqrt{2}} (\tilde{X} + \tilde{x}) \\ x_2 &= \frac{1}{\sqrt{2}} (\tilde{X} - \tilde{x}) \end{aligned} \right., \quad (\text{B5})$$

with an analogous relation for the variables p_1 and p_2 . The exponent in Eq. (B4) can now easily be expressed in terms of the new coordinates:

$$g(x_1, p_1, b)g(x_2, p_2, b) = \frac{1}{b} \pi^{-1/2} e^{-\frac{1}{2b^2}(\tilde{x}^2 + \tilde{X}^2) + \frac{2}{b}(\tilde{x}\tilde{p} + \tilde{X}\tilde{P}) - (\tilde{p}^2 + \tilde{P}^2)} = g(\tilde{X}, \tilde{P}, b)g(\tilde{x}, \tilde{p}, b). \quad (\text{B6})$$

By using the definition of the generating functions

$$g(\tilde{X}, \tilde{P}, b)g(\tilde{x}, \tilde{p}, b) = \sum_{N=0}^{\infty} \eta_N(\tilde{P})\phi_N(\tilde{X}, b) \sum_{n=0}^{\infty} \eta_n(\tilde{p})\phi_n(\tilde{x}, b), \quad (\text{B7})$$

the coefficients $\eta_N(\tilde{P})$ and $\eta_n(\tilde{p})$ can be expressed in terms of p_1 and p_2 :

$$\eta_N(\tilde{P}) = \sqrt{\frac{2^N}{N!}}\tilde{P}^N = \sqrt{\frac{1}{N!}}(p_2 + p_1)^N = \sqrt{\frac{1}{N!}} \sum_{M=0}^N \binom{N}{M} p_1^{N-M} p_2^M, \quad (\text{B8})$$

$$\eta_n(\tilde{p}) = \sqrt{\frac{2^n}{n!}}\tilde{p}^n = \sqrt{\frac{1}{n!}}(p_1 - p_2)^n = \sqrt{\frac{1}{n!}} \sum_{m=0}^n (-1)^{n+m} \binom{n}{m} p_1^m p_2^{n-m}. \quad (\text{B9})$$

The product of generating functions Eq. (B7) then reads

$$\sum_{n,N=0}^{\infty} \phi_N(\tilde{X}, b)\phi_n(\tilde{x}, b) \sqrt{\frac{1}{N!n!}} \sum_{M=0}^N \sum_{m=0}^n (-1)^{n+m} \binom{N}{M} \binom{n}{m} p_1^{N-M+m} p_2^{M+n-m}. \quad (\text{B10})$$

With the introduction of the auxiliary indices:

$$n_1 = N - M + m \quad \text{and} \quad n_2 = M + n - m, \quad (\text{B11})$$

the product Eq. (B10) can be rewritten in the form:

$$\begin{aligned} g(\tilde{X}, \tilde{P}, b)g(\tilde{x}, \tilde{p}, b) &= \sum_{n_1, n_2=0}^{\infty} p_1^{n_1} p_2^{n_2} \sum_{n, N=0}^{\infty} \phi_N(\tilde{X}, b)\phi_n(\tilde{x}, b) \sqrt{\frac{1}{N!n!}} \times \\ &\times \sum_{M=0}^N \sum_{m=0}^n (-1)^{n+m} \binom{N}{M} \binom{n}{m} \delta_{n_1, N-M+m} \delta_{n_2, M+n-m}. \end{aligned} \quad (\text{B12})$$

One of the Kronecker symbols can be used to eliminate the sum over M :

$$\begin{aligned} g(\tilde{X}, \tilde{P}, b)g(\tilde{x}, \tilde{p}, b) &= \sum_{n_1, n_2=0}^{\infty} p_1^{n_1} p_2^{n_2} \sum_{n, N=0}^{\infty} \phi_N(\tilde{X}, b)\phi_n(\tilde{x}, b) \sqrt{\frac{1}{N!n!}} \delta_{n_1+n_2, N+n} \times \\ &\times \sum_{m=0}^n (-1)^{n+m} \binom{N}{N-n_1+m} \binom{n}{m}. \end{aligned} \quad (\text{B13})$$

A comparison with the equivalent relation for the product (cf. Eq. (B4))

$$g(x_1, p_1, b)g(x_2, p_2, b) = \sum_{n_1, n_2=0}^{\infty} p_1^{n_1} p_2^{n_2} \sqrt{\frac{2^{n_1+n_2}}{n_1!n_2!}} \phi_{n_1}(x_1, b)\phi_{n_2}(x_2, b), \quad (\text{B14})$$

leads to the final expression for the transformation of the product of HO wave functions:

$$\phi_{n_1}(x_1, b)\phi_{n_2}(x_2, b) = \sum_{N, n} M_{n_1 n_2}^{nN} \phi_N(\tilde{X}, b)\phi_n(\tilde{x}, b), \quad (\text{B15})$$

where $M_{n_1 n_2}^{nN}$ are the coefficients of the transformation

$$M_{n_1 n_2}^{nN} = \sqrt{\frac{n_1! n_2!}{n! N!}} \sqrt{\frac{1}{2^{N+n}}} \delta_{n_1+n_2, n+N} \sum_m (-1)^{n+m} \binom{N}{N-n_1+m} \binom{n}{m}. \quad (\text{B16})$$

For the calculation of matrix elements of the pairing interaction, the center-of-mass and relative coordinates are used

$$X \equiv \frac{1}{\sqrt{2}}(x_1 + x_2) = \frac{1}{\sqrt{2}}\tilde{X} \quad \text{and} \quad x \equiv x_1 - x_2 = \sqrt{2}\tilde{x}. \quad (\text{B17})$$

The HO wave functions are expressed in terms of X and x :

$$\phi_N(\tilde{X}, b) = \phi_N(\sqrt{2}X, b) = \frac{1}{\sqrt{b}} \mathcal{N}_n H_n \left(\sqrt{2}X/b \right) e^{-2x^2/2b^2} = \frac{1}{\sqrt{2}} \phi_N(X, B), \quad (\text{B18})$$

$$\phi_n(\tilde{x}, b) = \phi_n(x/\sqrt{2}, b) = \frac{1}{\sqrt{b}} \mathcal{N}_n H_n \left(x/\sqrt{2}b \right) e^{-x^2/4b^2} = \sqrt{2} \phi_n(x, b_r), \quad (\text{B19})$$

where we have defined the oscillator lengths $B = b/\sqrt{2}$ and $b_r = \sqrt{2}b$. Finally, the product of two HO wave functions expressed in terms of the center-of-mass and relative coordinates reads:

$$\phi_{n_1}(x_1, b)\phi_{n_2}(x_2, b) = \sum_{N, n} M_{n_1 n_2}^{nN} \phi_N(X, B)\phi_n(x, b_r). \quad (\text{B20})$$

-
- [1] M. Bender, P.-H. Heenen, and P.-G. Reinhard, *Rev. Mod. Phys.* **75**, 121 (2003).
 - [2] D. Vretenar, A. V. Afanasjev, G. A. Lalazissis, and P. Ring, *Phys. Rep.* **409**, 101 (2005).
 - [3] J. F. Berger, M. Girod, and D. Gogny, *Nucl. Phys. A* **428**, 23c (1984).
 - [4] J. F. Berger, M. Girod, and D. Gogny, *Comp. Phys. Comm.* **63**, 365 (1991).
 - [5] J. Meng, *Nucl. Phys. A* **635**, 3 (1998).
 - [6] T. Nikšić, P. Ring, and D. Vretenar, *Phys. Rev. C* **71**, 044320 (2005).
 - [7] Y. Tian, Z. Y. Ma, and P. Ring, *Phys. Lett. B* **676**, 44 (2009).
 - [8] Y. Tian, Z. Y. Ma, and P. Ring, *Phys. Rev. C* **79**, 064301 (2009).
 - [9] Y. Tian, Z. Y. Ma, and P. Ring, *Phys. Rev. C* **80**, 024313 (2009).

- [10] T. Duguet, T. Lesinski, Eur. Phys. J. ST **156**, 207 (2008).
- [11] T. Lesinski, T. Duguet, K. Bennaceur, and J. Meyer, Eur. Phys. J. A **40**, 121 (2009).
- [12] T. Nikšić, Z. P. Li, D. Vretenar, L. Próchniak, J. Meng, and P. Ring, Phys. Rev. C **79**, 034303 (2009).
- [13] M. Serra and P. Ring, Phys. Rev. C **65**, 064324 (2002).
- [14] G. A. Lalazissis, T. Nikšić, D. Vretenar, and P. Ring, Phys. Rev. C **71**, 024312 (2005).
- [15] N. Paar, D. Vretenar, E. Khan, and G. Coló, Rep. Prog. Phys. **70**, 691 (2007).
- [16] P. Ring and P. Schuck, *The Nuclear Many-Body Problem* (Springer-Verlag, Berlin, 1980).
- [17] G. A. Lalazissis, D. Vretenar, P. Ring, M. Stoitsov, and L. Robledo, Phys. Rev. C **60**, 014310 (1999).
- [18] G. Audi, A. H. Wapstra, and C. Thibault, Nucl. Phys. A **729**, 337 (2003).
- [19] J.-P. Delaroche, M. Girod, H. Goutte, and J. Libert, Nucl. Phys. A **771**, 103 (2006).
- [20] N. Schunck and J. L. Egido, Phys. Rev. C **78**, 064305 (2008).
- [21] S. Hilaire and M. Girod, Eur. Phys. J. A **33**, 237 (2007).
- [22] W. Long, P. Ring, N. Van Giai, and J. Meng, arXiv:0812.1103[nucl-th].
- [23] D. Vautherin and D. M. Brink, Phys. Rev. C **5**, 626 (1972).
- [24] J. Dobaczewski, H. Flocard, and J. Treiner, Nucl. Phys. A **422**, 103 (1984).
- [25] S. Karatzikos, A. V. Afanasjev, G. A. Lalazissis, and P. Ring, arXiv:0909.1233[nucl-th].
- [26] S. Gandolfi, A. Y. Illarionov, S. Fantoni, F. Pederiva, and K. E. Schmidt, Phys. Rev. Lett. **101**, 132501 (2009).
- [27] N. Kaiser, T. Nikšić, and D. Vretenar, Eur. Phys. J. A **25**, 257 (2005).
- [28] K. Hebeler, T. Duguet, T. Lesinski, and A. Schwenk, Phys. Rev. C **80**, 044321 (2009).
- [29] M. Abramowitz and I. A. Stegun, *Handbook of Mathematical Functions* (Dover Publications, New York, 1970).

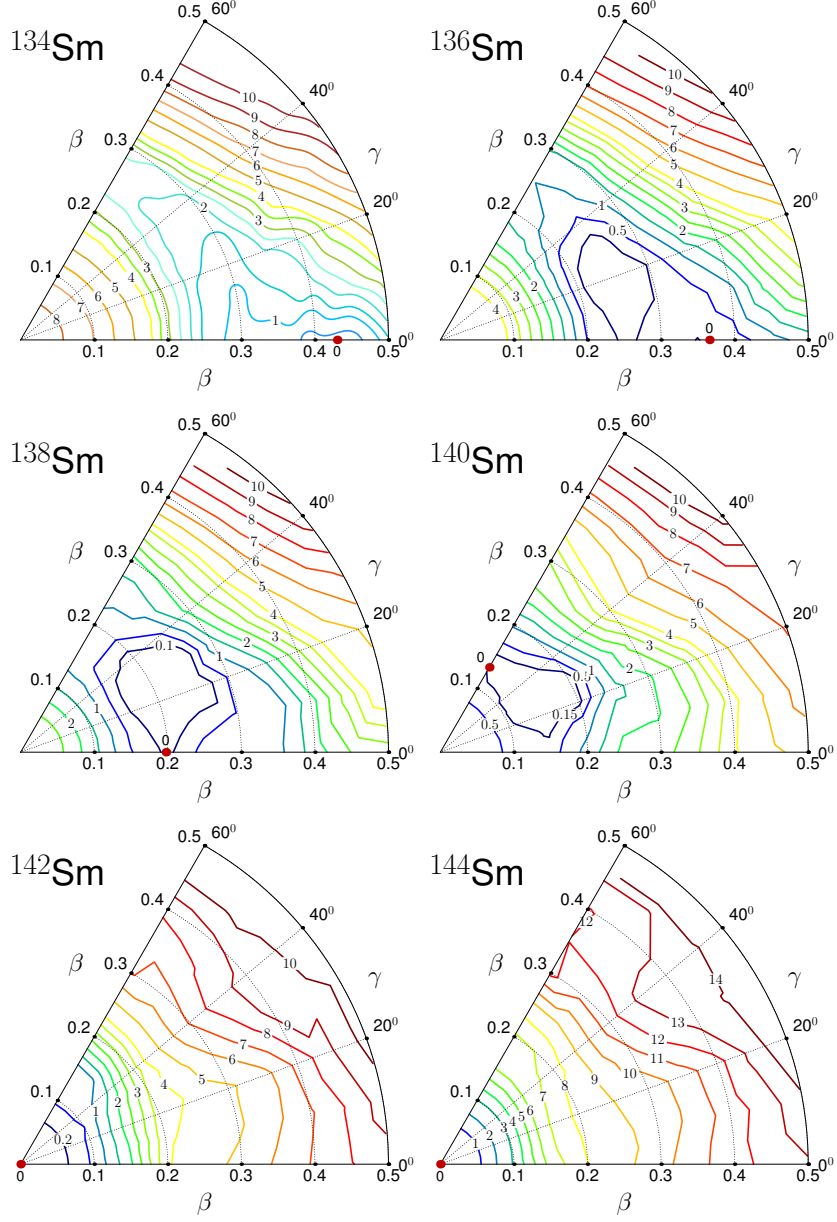


FIG. 1: (Color online) Self-consistent RHB triaxial quadrupole binding energy maps of the even-even isotopes $^{134-144}\text{Sm}$ in the $\beta - \gamma$ plane ($0 \leq \gamma \leq 60^\circ$). All energies are normalized with respect to the binding energy of the absolute minimum (red dot). The contours join points on the surface with the same energy (in MeV).

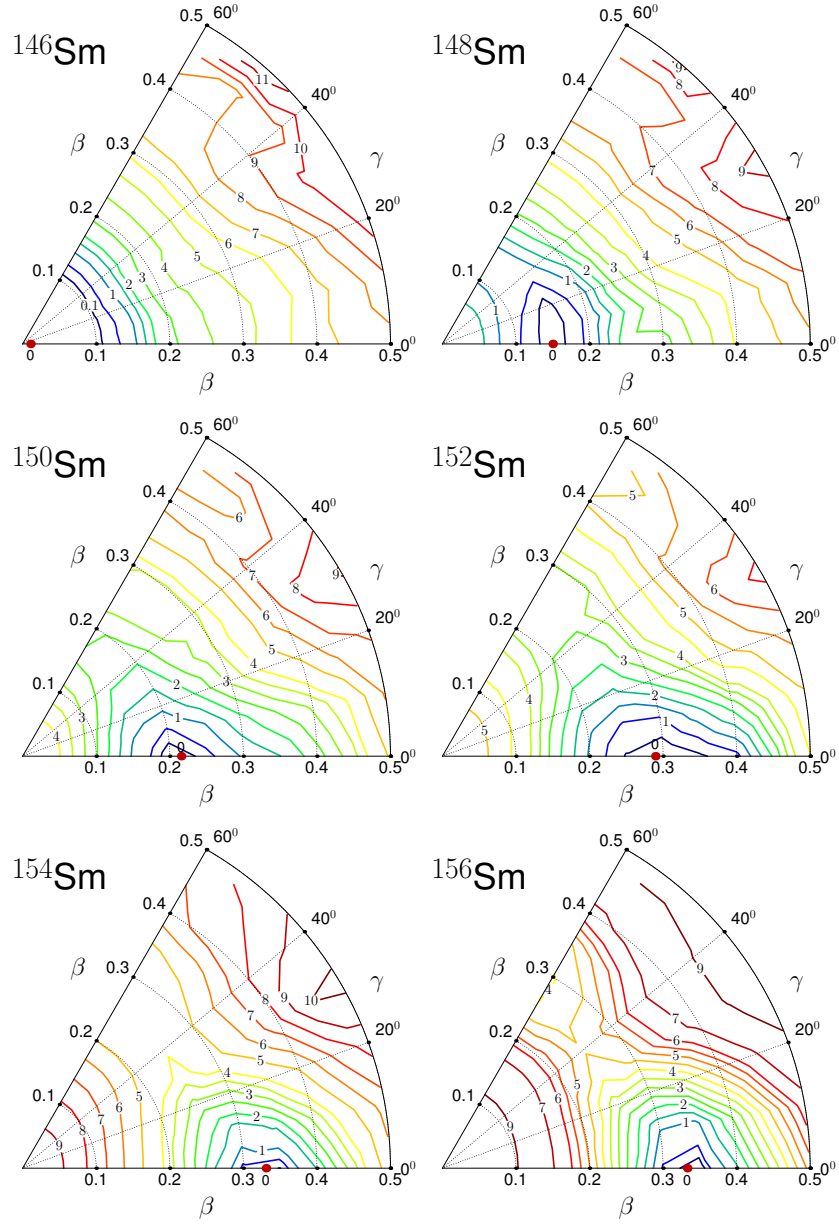


FIG. 2: (Color online) Same as Fig. 1, but for the isotopes $^{146}\text{--}^{156}\text{Sm}$.

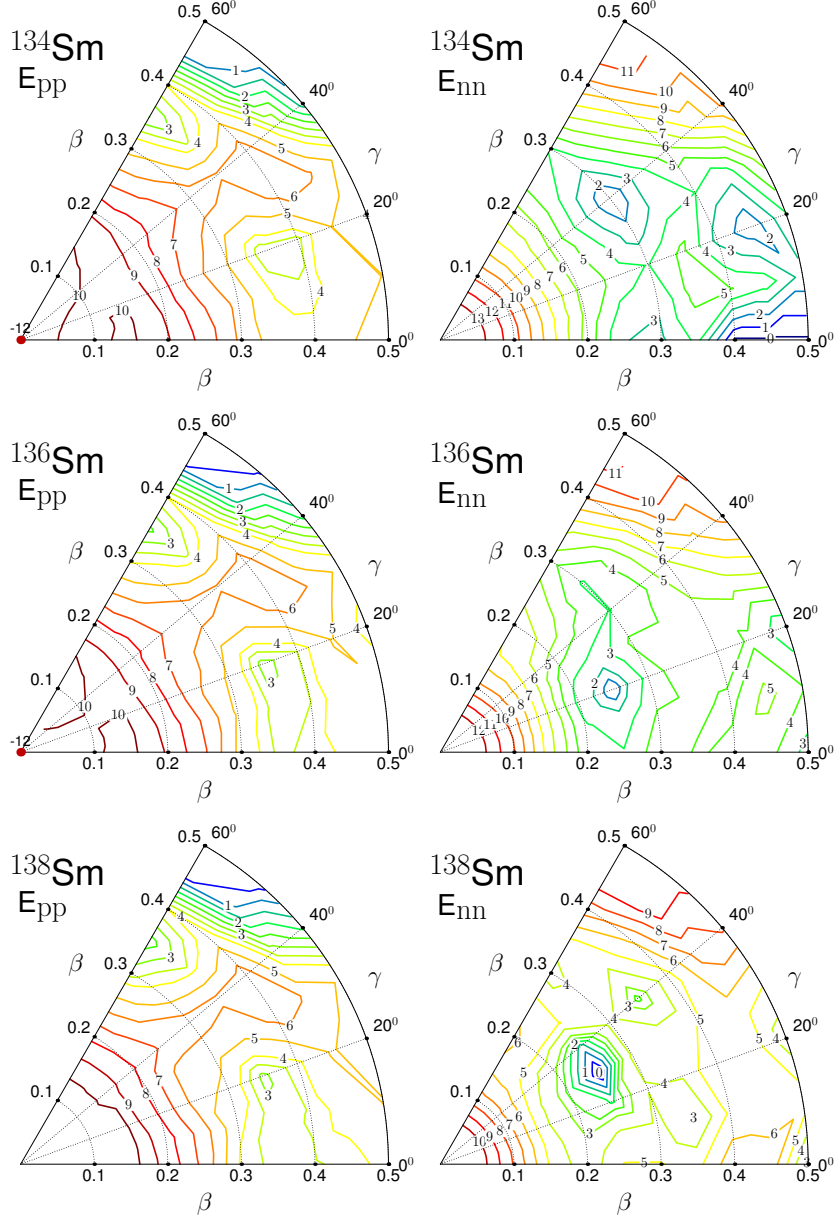


FIG. 3: (Color online) Proton (left column) and neutron (right column) pairing energies of $^{134,136,138}\text{Sm}$ in the $\beta - \gamma$ plane ($0 \leq \gamma \leq 60^\circ$). The contours join points on the surface with the same energy (in MeV).

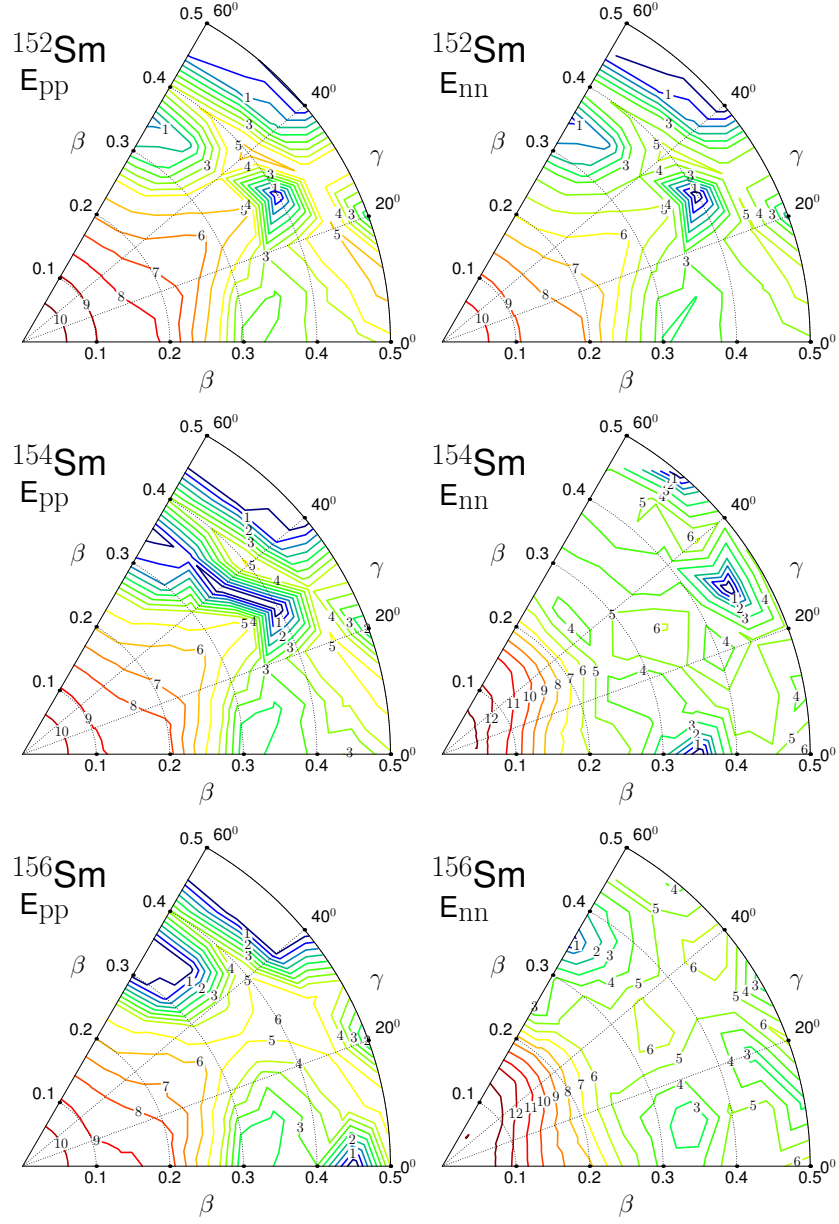


FIG. 4: (Color online) Same as Fig. 3, but for the isotopes $^{152,154,156}\text{Sm}$.

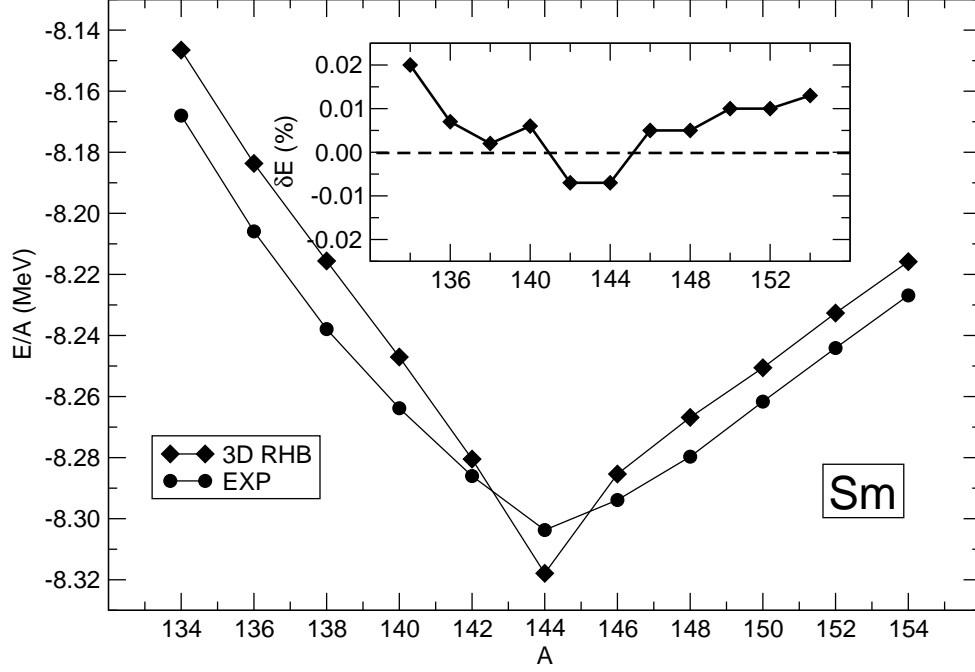


FIG. 5: Binding energy per nucleon for the sequence of Sm isotopes, calculated with the 3D RHB model and compared to data [18]. In the inset we display the relative differences (in percent): $(E^{\text{RHBZ}} - E^{\text{3DRHB}})/E^{\text{3DRHB}}$, between the binding energies calculated using the 3D RHB and the axial (RHBZ) relativistic Hartree-Bogoliubov models.

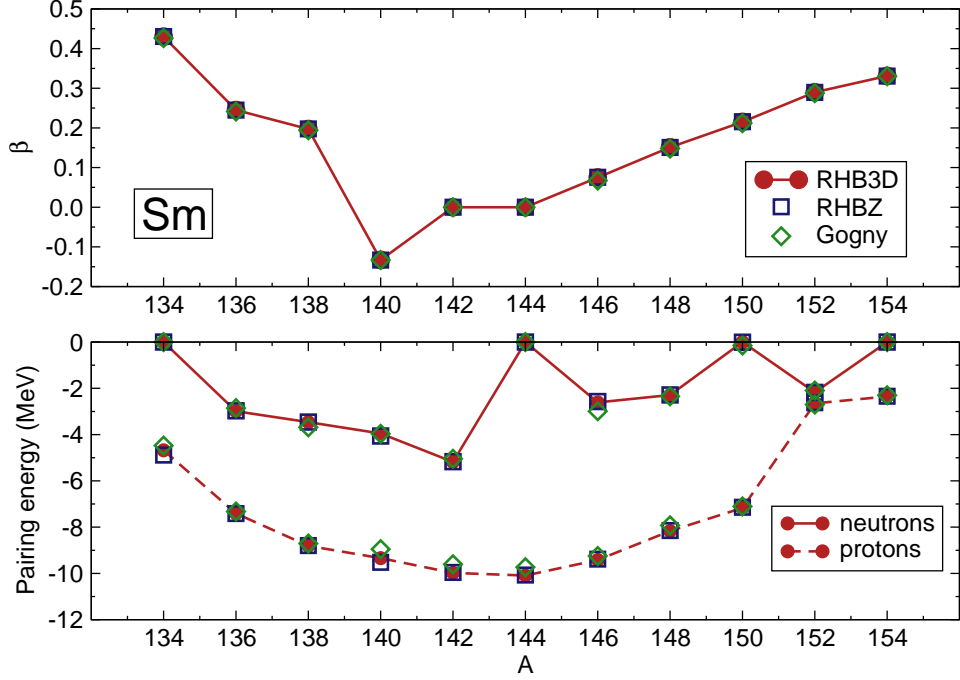


FIG. 6: (Color online) 3D RHB (filled circles) and axial (RHBZ) empty symbols) results for the self-consistent ground-state quadrupole deformations (upper panel), and neutron and proton pairing energies (lower panel) of even-A Sm isotopes. In calculations with axial symmetry both the separable force (squares) and the Gogny D1S force [4] (diamonds) are used.